

# Microstructural and Mechanical Properties of Nanostructured Chromium Nitride

Abishek.M<sup>1</sup>, Sukin Joshua.D<sup>1</sup>, vigneswaran.K<sup>1</sup>, ashwin.M.P<sup>1</sup>,UG scholar, Mechanical Engineering, Sri Lakshmi Ammal Engineering College, Chennai.

K.Kalaiselvan<sup>2</sup>, Assistant Professor,Dept of Mechanical, Sri Lakshmi Ammal Engineering College, Chennai.

<sup>12</sup>Anna University

<sup>12</sup>Sri Lakshmi Ammal Engg. College, Chennai, India

## 1. INTRODUCTION

### Chromium Nitride

Chromium nitride is a chemical compound of chromium and nitrogen with the formula CrN. It is very hard and extremely resistant to corrosion. It is an interstitial compound, with nitrogen atoms occupying the octahedral holes in the chromium lattice. Chromium forms a second interstitial nitride, dichromium nitride, Cr<sub>2</sub>N. CrN and Cr<sub>2</sub>N possess high melting point, low electrical resistivity, high microhardness and excellent abrasive wear, corrosion as well as oxidation resistance characteristics. Chromium nitride (CrN) is an attractive coating material due to its mechanical properties and refractory character. It is used as a protective coating material owing to its higher melting point, higher hardness, good thermal conductivity, and better corrosion resistance. Thin film of chromium nitride exists in cubic (CrN) and hexagonal (Cr<sub>2</sub>N) phases and its properties are therefore dependent on the crystalline phase. The growth of particular crystalline phases primarily depends on the deposition conditions, which can modify the thin film properties play an important role in applications, such as metallization and wear-resistant coatings. CrN thin films exhibit the semiconductor properties with a band gap of 0.7 eV, excellent spectral selectivity, and extremely low emittance, and thus may be used for solar selective absorbers.

CrN coating was developed to solve wear problems in special application areas where titanium based coatings were not successful. CrN resists adhesive wear, corrosion and oxidation. It is recommended for the machining of aluminium and copper, high temperature die casting applications, hot forging of brass and tooling for PVC moulding and extrusion. It is harder than conventional chrome plating and the PVD coating process used to apply CrN has no negative environmental side effects. CrN is used as a coating material for corrosion resistance and in metal forming and plastic moulding applications. CrN is often used on medical implants and tools. CrN is also a valuable component in advanced multicomponent coating systems, such as CrAlN, for hard, wear-resistant applications on cutting tools. Cutting and forming of copper, nickel, and monel metal. It exhibits enhanced thermal stability, oxidation resistance, excellent corrosion resistance and low internal stress of coating results in excellent adhesion under high loads.

The CrN coating was realized industrially by Balzers et al. are stable thermally until 700°C. observed that beyond 700°C, the Cr<sub>2</sub>O<sub>3</sub> appeared in CrN films and only this oxide remains present at 900°C. The oxidation of nitrides thin films is an important mechanism leading to the degradation of the mechanical properties at high temperatures . The chemical reaction between chromium nitride and oxygen gives the following equation:  $2\text{CrN} + (3/2)\text{O}_2 \rightarrow \text{Cr}_2\text{O}_3 + \text{N}_2$ . Thermal oxidation was much studied, for example, in the phase's transformations and that of the microstructures. The effect of the oxidation at high temperature and on different atmospheres on the mechanical properties of CrN system was studied by Chang et al.

In this study, Cr<sub>2</sub>N thin films are prepared by DC reactive magnetron sputtering at different substrate temperatures. The influence of growth temperature on the structure, surface morphology, and mechanical properties are examined.

### STRUCTURE

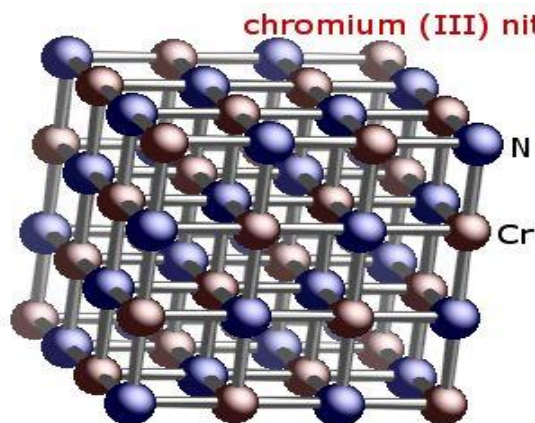


FIG.1

### PROPERTIES

Chemical formula	CrN
Molar mass	66.003 g/mol
Appearance	Black powder
Density	5.9 g/cm <sup>3</sup>
Melting point	1770 °C (decomp.)

Solubility in water	Insoluble
---------------------	-----------

### THIN FILM DEPOSITION TECHNIQUES

Many techniques are available for thin film deposition. Physical processes and chemical processes are the two main techniques used to produce thin film of metal oxides on the suitable substrates. The physical processes are mainly based on evaporation and sputtering. In the process of evaporation, where thermal energy is used to transform material from solid or liquid phase to the vapor phase. The vapor phases are condensed to a solid phase on heated and unheated substrates whose surfaces have atomic level steps or imperfections. In evaporation, the difference in the vapour pressures pose problem of stoichiometry. On the other hand, target poisoning and arcing are the main drawbacks of reactive sputtering technique. The common deposition techniques are shown in Fig.2.

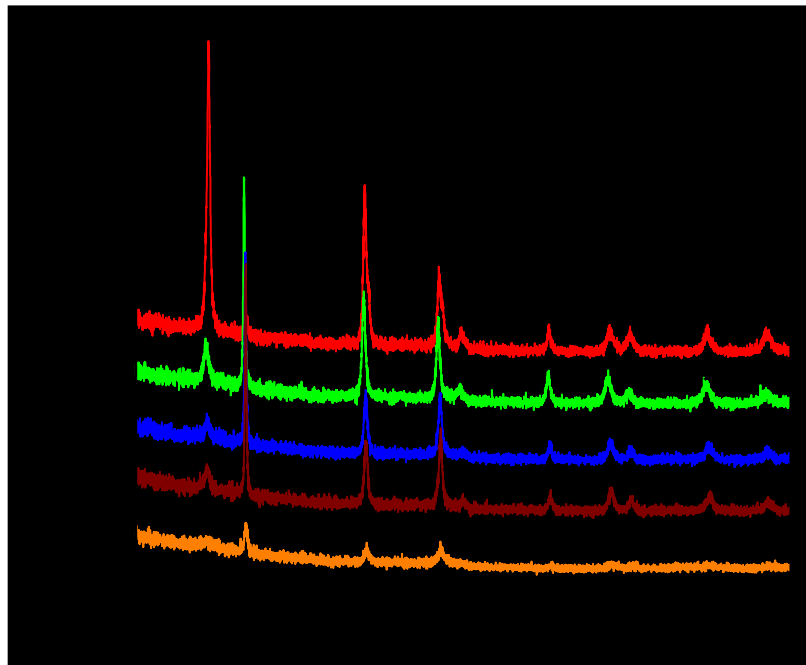


**FIG.2 Classification of the most common deposition techniques**

Procedures for depositing films are a very important set of processes since all of the layers above the surface of the wafer must be deposited. We can classify thin films into five groups: thermal oxides, dielectric layers, epitaxial layer, polycrystalline silicon, and metal films. Generally, the techniques used to deposit metals are physical, that is, they do not involve a chemical reaction. Processes used to deposit semiconducting and insulating layers often involve chemical reactions. This distinction, however, is changing. One of the areas currently being developed is the chemical deposition of metals. This module will cover techniques to generate metal films. Metal films such as aluminum and silicides are used to form low-resistance interconnections, Ohmic contacts, and rectifying metal-semiconductor barriers. The procedure to generate such films is called physical vapor deposition (PVD).

### **Pulsed laser deposition**

In the PLD process, several operating parameters, such as wavelength, fluence, repetition rate, energy per pulse, ambient gases, pressure, target to substrate distance and substrate temperature could be optimized to obtain films for specific application.

The schematic of the pulsed laser deposition system and the photograph of the PLD system used in the present investigations. PLD system mainly consists of a laser source and vacuum chamber. A target holder and substrate holder are housed in a vacuum chamber. High power laser is used as an external energy source to ablate materials to prepare thin films. The mechanism that leads to material ablation depends on laser characteristics, as well as the optical, topological and thermodynamic properties of the target. When the laser radiation is absorbed by a solid surface, electromagnetic energy is converted first into electronic excitation and then into thermal, chemical and even mechanical energy to cause evaporation, ablation, excitation, plasma formation and exfoliation.

The thin film formation in PLD generally can be divided into the following four stages:

- i. Laser radiation interaction with the target.
- ii. Dynamics of the ablation materials.
- iii. Deposition of the ablation materials with the substrate.
- iv. Nucleation and growth of a thin film on the substrate surface.

The nucleation and growth of crystalline films depends on many factors such as the density, energy, ionization degree and the type of the condensing material as well as the temperature and the physico-chemical properties of the substrate. The two main thermodynamic parameters for the growth mechanism are the substrate temperature  $T$  and the supersaturation  $D_m$ . They can be related by the following equation;

$$D_m = kT \ln(R/R_e)$$

where  $k$  is the Boltzmann constant,  $R$  is the actual deposition rate, and  $R_e$  is the equilibrium value at the temperature  $T$ .

### **SOL-GEL METHOD**

”Formation of an oxide network through polycondensation reactions of a molecular precursor in a liquid.”

A sol is a stable dispersion of colloidal particles or polymers in a solvent. The particles may be amorphous or crystalline. An aerosol is particles in a gas phase, while a sol is particles in a liquid. A gel consists of a three dimensional continuous network, which encloses a liquid phase. In a colloidal gel, the network is built from agglomeration of colloidal particles. In a polymer gel the particles have a polymeric sub-structure made by aggregates of sub-colloidal particles. Generally, the sol particles may interact by van der Waals forces or hydrogen bonds. A gel may also be formed from linking polymer chains. In most gel systems used for materials synthesis, the interactions are of a covalent nature and the gel process is irreversible. The gelation process may be reversible if other interactions are involved. The idea behind sol-gel synthesis is to “dissolve” the compound in a liquid in order to bring it back as a solid in a controlled manner. Multi component compounds may be prepared with a controlled stoichiometry by mixing sols of different compounds. The sol-gel method prevents the problems with co-precipitation, which may be inhomogeneous, be a gelation reaction. Enables mixing at an atomic level. Results in small particles, which are easily sinterable. The sol-gel method was developed in the 1960s mainly due to the

need of new synthesis methods in the nuclear industry. A method was needed where dust was reduced (compared to the ceramic method) and which needed a lower sintering temperature. In addition, it should be possible to do the synthesis by remote control.

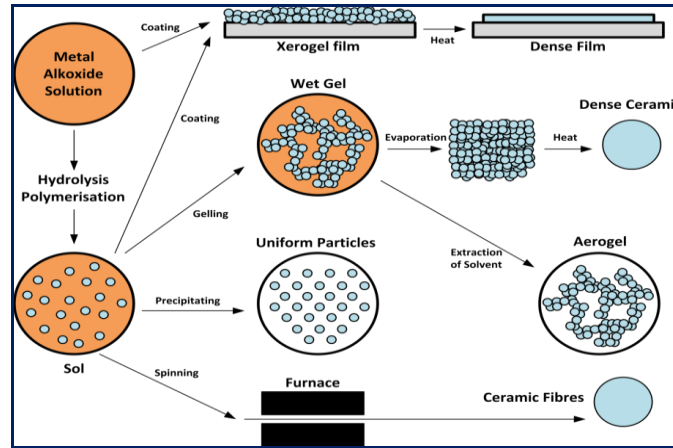


FIG.3

## II. MAJOR FORMAT GUIDELINES

### EXPERIMENTAL DETAILS

The main physical phenomenon involved in the sputtering technique is the momentum transfer between energetic atomic-sized particles (usually ions of noble gases) and the atoms of the surface of the material (target). During the interchange of momentum, many effects can be produced on the elastic and inelastic collisions; in the first kind of collision, mainly reflected particles can be found (neutrals, ions of the target and the gas). In the second kind, the collisions can present secondary electrons, UV/visible photons, X-ray and implanted particles.

The momentum-transfer theory for physical sputtering was proposed early on, but was replaced by the “hot-spot” theory, in which the process of thermal vaporization is involved. The confusion about the physical process present in sputtering has only been overcome thanks to the work of Gunthersshulze in the 1920’s and 30’s and Wehner *et al.* in the 1950’s and 60’s, who demonstrated that the effects produced in sputtering could only be explained by the momentum transfer theory. These effects can be summarized as:

1. The sputtering yield (ratio of atoms sputtered to the number of high-energy incident particles) depends on the mass of the bombarding particle as well as their energy. The sputtering yield is sensitive to the angle-of-incidence of the bombarding particle. There is a “threshold energy” below which sputtering does not occur no matter how high the bombarding flow.
2. Many sputtering atoms have kinetic energies much higher than those of thermally evaporated atoms.
3. Atoms ejected from single crystals tend to be ejected along the directions of the closepacked planes in the crystal.
4. In a polycrystalline material, some crystallographic planes are sputtered faster than are others.
5. Atoms sputtered from the alloy’s surface are deposited in the ratio of the bulk composition, not their relative vapor pressure, as in the case of thermal vaporization.

6. Sputtering yields decrease at very high energies because the ions lose much of their energy far below the surface.
  7. The sputtering yield is rather intensive to the temperature of the sputtering target.
  8. There is no sputtering by electrons even at very high temperature.
  9. The secondary electron emission by ion bombardment is low, whereas high rates from thermo electron emission would be expected if high temperatures were present.
- Effects 1 through 7 above are important for the growth of films by sputter deposition. This is particularly true for low pressure (<5 m Torr).

## **Working principle**

### Sputtering

Sputter deposition is a physical vapor deposition (PVD) method of thin film deposition by sputtering. This involves ejecting material from a "target" that is a source and deposited onto a "substrate" such as a silicon wafer or metal substrates.

## **DEPOSITION PARAMETERS**

- RF/DC (Plasma type)
- RF/DC Power
- Argon gas pressure
- Target-substrate spacing
- Ambient gas/pressure
- Substrate temperature
- Deposition rate ( $\text{\AA}/\text{sec}$ )

## **RF/DC Sputtering**

Depending on the target material either RF or DC sputtering may be used. If the target material is a conductor, a constant voltage can be used to accelerate the ions to the desired bombarding velocity. As the ions strike the surface, the resulting charges can move freely about the material to prevent any charge buildup. However, if the material is an insulator, the conduction bands will not allow free charge movement. As the ions strike the surface, their charge will remain localized and over time the charge will build up, making it impossible to further bombard the surface. In order to prevent this, alternating current is used at a frequency above 50 KHz. A high frequency is used so that the heavy ions cannot follow the switching fast enough and only electrons hit the surface to neutralize charge.

## **Magnetron sputtering can be done in either DC or RF modes**

### DC sputtering:

- DC sputtering is done with conducting materials.

- If target is non-conducting material, the positive charge will build up on target material and stops sputtering

#### RF sputtering:

- Both conducting and non-conducting materials can be sputtered.
- Higher sputter rate at lower pressure.

### **ADVANTAGES OF MAGNETRON SPUTTERING**

Here magnets are used to increase the percentage of electrons that take part in ionization events, increase probability of electrons striking Argon, increase electron path length, so the ionization efficiency is increased significantly

The primary advantages are

1. Wide range of materials (Metals, Semiconductors and Ceramics)
2. High deposition rates,
3. Ease of sputtering any metal, alloy or compound,
4. High-purity films
5. Extremely high adhesion of films,
6. Ability to coat heat-sensitive substrates,
7. Ease of automation, and
8. Excellent uniformity on large-area substrates
9. Low pressure operation
10. Elimination of secondary electrons on substrates
11. Good control over reactive sputtering.

### **APPLICATIONS**

- Tribological coatings for automobile components and corrosion resistant coatings
- Optical coatings
- Protective coatings for lenses, mirrors and TCO coatings for displays
- Decorative coating
- Data storage – CDs and DVDs
- Semiconducting industry, metallisation, barrier layers, display circuitry, discrete components.
- Deposit thin films of various materials in integrated circuit processing

### **CHARACTERIZATION TECHNIQUES**

#### **Thickness measurement: Dektak Profilometer**

Thickness of the films were measured using Dektak Profilometer (Dektak 6M-Stylus profiler by Veeco, USA). The stylus method comprises a fine diamond tip with a radius of 0.7 to 2  $\mu\text{m}$  which is pressed on to the surface with a pressure of 500  $\text{kP}/\text{cm}^2$  (corresponding to a tip mass of only 0.1 g) and dragged along the surface of the substrate. The vertical movement of the tip, caused by irregularities of the surface, is converted to an electrical signal, which is then amplified and recorded. The results obtained



by the stylus are in good agreement with other methods. It is capable of measuring step heights between 100 Å and ~50 microns with a resolution of 10 Å.

### X-Ray Diffraction

X-ray diffractometers consist of three basic elements: an X-ray tube, a sample holder, and an X-ray detector. X-rays are generated in a cathode ray tube by heating a filament to produce electrons, accelerating the electrons toward a target by applying a voltage, and bombarding the target material with electrons. When electrons have sufficient energy to dislodge inner shell electrons of the target material, characteristic X-ray spectra are produced. Copper is the most common target material for single-crystal diffraction, with  $\text{CuK}\alpha$  radiation = 1.5418 Å.

These X-rays are collimated and directed onto the sample. As the sample and detector are rotated, the intensity of the reflected X-rays is recorded.

### Working Principle

XRD analysis is based on constructive interference of monochromatic X-rays and a crystalline sample: The X-rays are generated by a cathode ray tube, filtered to produce monochromatic radiation, collimated to concentrate, and directed toward the sample.

The interaction of the incident rays with the sample produces constructive interference (and a diffracted ray) when conditions satisfy Bragg's Law ( $n\lambda=2d \sin \theta$ ).

The characteristic x-ray diffraction pattern generated in a typical XRD analysis provides a unique "fingerprint" of the crystals present in the sample.

Braggs law

$$2d\sin\theta=n\lambda$$

where  $n$  is a positive integer and  $\lambda$  is the wavelength of incident wave

The observed diffraction line profiles in a diffraction pattern are distribution of intensities  $I(2\theta)$  defined by several parameters [Cullity, 1978],

- i. The reflection angle position  $2\theta$  at the maximum intensity
- ii. The dispersion of the distribution, full-width at half maximum and integral breadth
- iii. The line shape factor
- iv. The integrated intensity

The crystalline phases and orientation of all the thin films of the present work were identified by matching the XRD peaks with those given in the data base (JCPDS). In this study INEL XRG – 3000 X-ray Diffractometer (40 kV and 30 mA, Inel, France) with  $\text{Cu-K}\alpha_1$  radiation ( $\lambda = 1.54056 \text{ \AA}$ ) equipped with curved position sensitive detector (CPSD) was used for the present analysis. The x-ray scans were performed with a glancing angle of  $5^\circ$  and  $2\theta$  values ranging from  $20^\circ$  to  $90^\circ$  with a typical step size of about  $0.02^\circ$ .

### Crystallite Size Analysis

The lattice parameter of bulk and thin film at various parameters were refined by the method of least square fit using the Unit Cell Program. The crystallite size broadening profile, which frequently dominates the reflection, could be represented by the Gaussian function.



The crystallite size can be determined from the broadening of corresponding x-ray peaks by Scherrer's equation [Cullity, 1978],

$$D = \frac{k\lambda}{\beta \cos \theta}$$

where  $\beta = \sqrt{B^2 - b^2}$  and D is the crystallite size,  $\lambda$  is the wavelength of X-ray radiation ( $\text{CuK}\alpha_1 = 1.5406 \text{ \AA}$ ),  $\theta$  is the diffraction angle and k is Scherrer's constant (assuming 0.9, since the particles are spherical). B is the experimental FWHM and b is the instrumental broadening for the standard Si powder. This is a generally accepted method to estimate the mean crystallite size.

### Scanning Electron Microscope

A **scanning electron microscope (SEM)** is a type of electron microscope that produces images of a sample by scanning it with a focused beam of electrons. The electrons interact with atoms in the sample, producing various signals that contain information about the sample's surface topography and composition. The electron beam is generally scanned in a raster scan pattern, and the beam's position is combined with the detected signal to produce an image. SEM can achieve resolution better than 5 nanometer. Specimens can be observed in high vacuum, in low vacuum, in wet conditions (in environmental SEM). The most common SEM mode is detection of secondary electrons emitted by atoms excited by the electron beam. The number of secondary electrons that can be detected depends, among other things, on specimen topography. By scanning the sample and collecting the secondary electrons that are emitted using a special detector, an image displaying the topography of the surface is created.

### SEM ADVANTAGES

SEMs have a variety of applications in a number of scientific and industry-related fields, especially where characterizations of solid materials is beneficial. This instrument works fast, often completing SEI, BSE and EDS analyses in less than five minutes. In addition, the technological advances in SEMs are also easy to operate with the proper training and advances in computer technology and associated software make operation user-friendly. In the present study all the films are nonconducting, because of that, very thin gold layer of about 10 nm is sputter coated for conduction. The surface morphology and compositions were analyzed by using XL30 ESEM Philips scanning electron microscope (SEM) with resolution of 5 nm fitted with X-ray Energy Dispersive Analyzer.

**Mechanical Properties –Nanoindentation** Indentation techniques such as the Knoop and Vickers techniques are commonly used to measure micro-scale hardness of materials. The microhardness indentation measurement is a simple, reproducible, and cheap method, which is often used for the characterization of surface for mechanical applications. These techniques are not sufficient for many thin-film studies due to the large required material thickness. Measuring the elastic and plastic properties of thin films is always the first critical step to analyze their mechanical integrity and among alternative techniques. To allow for ultra-thin film probing, nano-indentation techniques were developed. Nanoindentation employs a diamond tip with a sub 0.01  $\mu\text{m}$  radius. The specimen was put on the horizontal holder with a microscope directly located above the selected area. The conditions of the measurement are following: at a room temperature (25°C) and at a relative humidity around 55 %. With some basic knowledge of the shape of the indentation and the indenter geometry this data can be used to

calculate hardness and reduced modulus of the film. With knowledge of the Poisson's ratio for the tip and sample and the elastic modulus of the tip, the elastic modulus of the sample can be calculated.

The nanohardness,  $H_n$ , is defined as follows :

$$H_n \text{ (GPa)} = \frac{P_{max}}{A_c}$$

where  $P_{max}$  is the maximum indentation load and  $A_c$  is the projected contact area at peak load. The contact area is calculated from the tip shape of the indenter and the corresponding contact depth.

In the present study, the maximum indentation loads of the specimens were 3000  $\mu\text{N}$ . The indenter had a Berkovich diamond tip and indentations of 500–1000 nm were produced. Nanoindentation tests were performed with about five scans in each  $90 \times 90\text{-}\mu\text{m}$  area. Nanohardness can be measured directly on the tool surface without breaking the surface, because the indentation is too small to cause any damage. The load– displacement experiments were repeated on 6 independent locations of the surface of each specimen. The indentation depth is only 1/10 th of the total film thickness in order to avoid the substrate effect.

## LITERATURE SURVEY

Lu et al deposited the chromium nitride coatings on metal surface by physical vapour deposition processes. This study is undertaken on the surface of mild steel by DC magnetron sputtering process, which offers an efficient method to form chromium nitride coatings on metal surfaces. The process was carried out in the temperature range of 1000 °C–1100 °C. The microstructures of the coatings were characterized using scanning electron microscopy (SEM) and energy dispersive spectroscopy (EDS). The structure of the coatings was analyzed by X-ray diffraction (XRD). The effects of processing temperature and time on the microstructures of the coatings are discussed.

This work presents the effect of substrate bias voltage on the results of the deposition of chromium nitride coatings on HS6-5-2 steel substrates on the front and reverse side of the substrates with respect to the cathode by cathodic arc evaporation. The deposition was carried out at a fixed nitrogen pressure 3.0 Pa and the negative substrate bias voltages: 70, 150, 300 V. The difference in the deposition rate, phase and chemical composition, amount and dimensional distribution of macroparticles and surface roughness were studied. It was found that the coatings obtained on the reverse side of the substrate were characterized by a nearly 3-times smaller amount of surface defects, more than twice the lower surface roughness and similar chemical composition as the coatings deposited on the front side of the substrate. The measurements have shown that the hardness of the coatings obtained on both sides of the substrate is comparable, and decreases with increasing the negative substrate bias voltage .

Large diameter total hip replacements using polyethylene liners have been proposed due to low wear and oxidative stability observed in the material. A ceramic chromium nitride (CrN) coating on a metal head may be an alternative bearing surface, maintaining low polyethylene wear and minimising cobalt release. Vitamin-E blended highly cross-linked polyethylene liners, paired with electron beam physical vapour deposited (EBPVD) CrN coated and uncoated CoCrMo heads were tested in a hip simulator. Under standard conditions no difference was observed in polyethylene wear rates (9.2 and 9.5  $\text{mm}^3/\text{mc}$ ) but the coating prevented cobalt release. Alumina particles produced substantial damage on the uncoated heads

but did not damage the coated heads. This CrN coating may have the potential to reduce clinical wear allowing for large diameter components .

## REFERENCES

- [1] Z.B. Zhao, Z.U. Rek, S.M. Yallisove, J.C. Bilello, *Thin Solid Films* 472, 96 (2005).
- [2] J. Lin, Z.L. Wu, X.H. Zhang, B. Mishra, J.J. Moore, and W.D. Sproul, A comparative study of CrNx coatings synthesized by dc and pulsed dc magnetron sputtering, *Thin Solid Films*, 517(2009), No. 6, p. 1887.
- [3] Z.B. Qi, B. Liu, Z.T. Wu, F.P. Zhu, Z.C. Wang, and C.H. Wu, A comparative study of the oxidation behavior of Cr<sub>2</sub>N and CrN coatings, *Thin Solid Films*, 544(2013), p. 515.
- [4] B.W. Karr, I. Petrov, D.G. Cahill, and J.E. Greene, Morphology of epitaxial TiN (001) grown by magnetron sputtering, *Appl. Phys. Lett.*, 70(1997), p. 1703.
- [5] S. Logothetidis, P. Patsalas, K. Sarakinos, C. Charitidis, and C. Metaxa, The effect of crystal structure and morphology on the optical properties of chromium nitride thin films, *Surf. Coat. Technol.*, 180-181(2004), p. 637.
- [6] M. Sikkens, A.A.M.T. van Heereveld, E. Vogelzang, and C.A. Boose, The development of high performance, low cost solar-selective absorbers, *Thin Solid Films*, 108(1983), No. 3, p. 229. [7] D. Gall, C.S. Shin, R.T. Haasch, I. Petrov, and J.E. Greene, Band gap in epitaxial NaCl-structure CrN (001) layers, *J. Appl. Phys.*, 91(2002), p. 5882
- [8] J. Vetter, *Surf. Coat. Technol.* 76, 719 (2005)
- [9] B. Balzers, [www.balinit.balzers.com](http://www.balinit.balzers.com), 21 March (2001).
- [10] J. Almer, M. Oden, L. Hultman, G. Håkansson, *J. Vac. Sci. Technol. A* 18, 121 (2000).
- [11] E. Huber, S. Hofmann, *Surf. Coat. Technol.* 68-69, 64 (1994).
- [12] P. Panjan, B. Navin<sup>2</sup>ek, A. Cvelbar, A. Zalar, I. Milo<sup>2</sup>ev, *Thin Solid Films* 281-282, 298 (1996).
- [13] F.-H. Lu, H.-Y. Chen, *Thin Solid Films* 398-399, 368 (2001).
- [14] W.P. Hsieh, C.C. Wang, C.H. Lin, F.S. Shieu, *J. Electrochem. Soc.* 149, B234 (2002).
- [15] K.-L. Chang, S.-C. Chung, S.-H. Lai, H.-C. Shih, *Appl. Surf. Sci.* 236, 406 (2004).

## Results and Discussion

### Thickness measurement

The thickness of the CrN coatings on mild steel is measured by using the Stylus profilometer and is found to be in the range of 1.6-1.9  $\mu\text{m}$ .

